Journal of the Serbian Society for Computational Mechanics / Vol. 19 / No. 1, 2025 / pp 104-114 / review paper
(10.24874/jsscm.2025.19.01.03)

CONSTITUTIVE MODELS FOR SOIL AND ROCK

Dragan Rakić [1*] [0000-0001-5152-5788], **Miroslav Živković** [1] [0000-0002-0752-6289]

[1] University of Kragujevac, Faculty of engineering, Kragujevac, Serbia
e-mail: **drakic@kg.ac.rs**
**corresponding author*

Abstract

The paper presents the procedure of implicit stress integration for constitutive models for soil and rock. The theoretical basis of Mohr-Coulomb, Matsuoka-Nakai, Hoek-Brown and Hyperbolic soil constitutive models are presented. Stress integration was performed using the theory of incremental plasticity. The general procedure of implicit stress integration of the mentioned constitutive models is shown, as well as the algorithm for their implementation. The presented constitutive models are implemented in the general-purpose program PAK intended for static and dynamic, linear and non-linear analysis of structures. Verification of the implemented algorithms are performed using test examples.

Keywords: Constitutive modeling, soil and rock, incremental plasticity, stress integration, PAK

1. Introduction

Modeling the mechanical behavior of soil and rock is one of the key tasks in the field of computational geomechanics, since these materials are highly nonlinear, heterogeneous and subject to complex deformation and fracture mechanisms. Constitutive models, which describe the relationship between stress and strain in a material, are necessary for reliable numerical analyzes in engineering practice. Depending on the type of material, loading conditions and accuracy requirements, different constitutive models are used such as Mohr-Coulomb, Matsuoka-Nakai, Hyperbolic soil model and Hoek-Brown (Balmer, 1952; Matsuoka, et al., 1994; Maksimović, 2008; Hoek, et al., 2002), which cover a wide range of behavior, from granular soil types to massive rock masses.

One of the key aspects in the numerical implementation of constitutive models is the stress integration procedure, that is, the way in which the state of stress is determined for a given strain increment. Implicit stresses integration, based on the incremental plasticity theory, enables stable and reliable solving of nonlinear problems, especially in cases where there is significant plastic yielding or when it is necessary to simulate the behavior of the material until failure. In contrast to explicit methods, implicit procedures provide greater numerical stability, especially for large time steps and complex shapes of yield surfaces.

With the aim of practical application of these models, appropriate algorithms were developed for their implementation in the general program package PAK (Kojić, et al., 2011), intended for static and dynamic analysis of structures. The PAK program enables non-linear analysis of various types of structures and materials, including soil and rock. The implementation of

advanced constitutive models with implicit stress integration significantly expands the capabilities of the software package and enables its application in complex geotechnical analyses.

The aim of this paper is to present the theoretical foundations and numerical implementation of selected constitutive models for soil and rock, with a focus on the implicit stress integration procedure. The paper is organized in such a way that the second chapter provides an overview of the theoretical foundations of the selected constitutive models, the third chapter presents the general implicit integration procedure, while the fourth chapter presents the numerical implementation of the presented algorithms in the PAK software. The fifth chapter contains the verification of the implemented models through the simulation of triaxial tests and direct shear tests, on one finite element model.

2. Theoretical Background of Constitutive Models

2.1 Mohr-Coulomb Model

The Mohr-Coulomb constitutive model is one of the most commonly used models for the numerical simulation of soil mechanical behavior (Balmer, 1952; Smith & Griffiths, 2004). The model defines a direct dependence of the shear stress at failure τ_f on the normal stress σ:

$$\tau_f = c + \sigma \tan\phi \tag{1}$$

using two material parameters: cohesion c and angle of internal friction in the material ϕ.

The yield surface of the Mohr-Coulomb model in the principal stresses space has the shape of an irregular six-sided pyramid whose axis coincides with the hydrostatic axis, which is shown in **Fig. 1**.

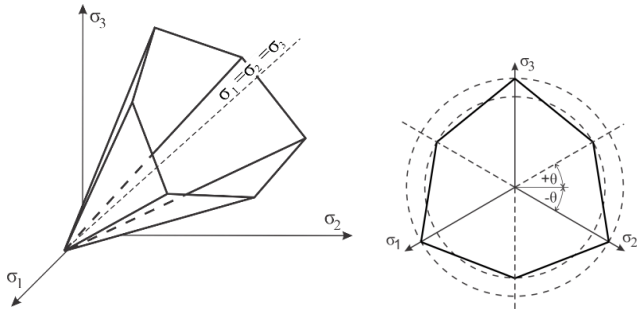

Fig. 1. Yield surface of the Mohr-Coulomb constitutive model

The yield surface equation of this constitutive model is a function of the stress invariant i (Smith & Griffiths, 2004) and reads

$$f = \frac{I_1}{3}\sin\phi + \sqrt{J_{2D}}\left(\cos\theta - \frac{1}{\sqrt{3}}\sin\theta\sin\phi\right) - c\cos\phi \tag{2}$$

In the case of a non-associative flow condition, the plastic potential function (g) differs from the yield function (f). These two functions have the same form, but the angle of dilatancy ψ

is introduced instead of the angle of internal friction in the material ϕ. The quantity θ in equation (2) represents the Lode angle (Balmer, 1952), which is defined by applying the stress invariant.

1.1 Matsuoka-Nakai Model

In the case of the Mohr-Coulomb yield surface, the numerical problem of determining the derivative of the yield function and the plastic potential function at the boundary values of the Lode's angle ($\theta = \pm 30^{\circ}$) often arises. In order to avoid this problem, the smooth Matsuoka-Nakai equation on the yield surface was introduced (Matsuoka & Nakai, 1974), which does not contain discontinuities in the yield surface, is a function of the stress invariant I_1, I_2, I_3 and reads

$$f = I_3 + \frac{\cos^2 \phi}{9 - \sin^2 \phi} I_1 I_2 \tag{3}$$

The yield surface of the Matsuoka-Nakai model in the space of principal stresses, in parallel with the yield surface of the Mohr-Coulomb model, is shown in **Fig. 2**.

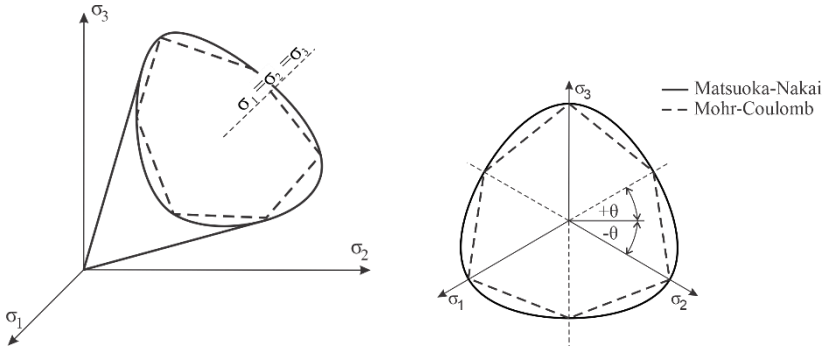

Fig. 2. Yield surface of the Matsuoka-Nakai constitutive model

In the case of a non-associative yield condition, the equation of the plastic potential (g) differs from the equation of the yield surface (f), for the angle of dilatancy ψ instead of the angle of internal friction in the material ϕ.

The yield surface equation (3) does not contain material cohesion c, so in order to take it into account, it is necessary to correct the stress tensor (Matsuoka, et al., 1994), in accordance with the equation

$$\sigma_{ij}^{*} = \sigma_{ij} - \sigma_0 \delta_{ij} \tag{4}$$

where δ_{ij} is the Kronecker operator, while $\sigma_0 = c\, ctg\, \phi$ represents the maximum tensile stress.

Generalized Hoek-Brown model

The generalized Hoek-Brown constitutive model, intended for the simulation of the mechanical behavior of the rock mass, defines the dependence between the highest and the lowest principal stress (Hoek, et al., 2002; Hoek, 2007)

$$\sigma_1 = \sigma_3 + \sigma_{ci}\left(m_b \frac{\sigma_3}{\sigma_{ci}} + s\right)^a \tag{5}$$

The equation of the yield surface is a function of the stress invariants I_1 and J_{2D}

$$f = \frac{I_1}{3} m_b \sigma_{ci}^{\left(\frac{1}{a}-1\right)} - s\sigma_{ci}^{\frac{1}{a}} + 2^{\frac{1}{a}}\left(\sqrt{J_{2D}}\cos\theta\right)^{\frac{1}{a}} + m_b\sqrt{J_{2D}}\,\sigma_{ci}^{\left(\frac{1}{a}-1\right)}\left(\cos\theta - \frac{1}{\sqrt{3}}\sin\theta\right) \tag{6}$$

The yield surface of this model in the space of main stresses is shown in Fig. 3.

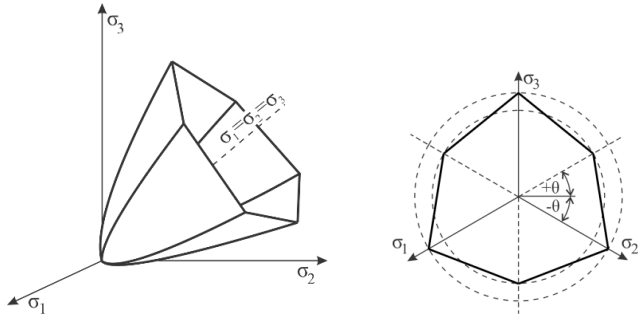

Fig. 3. Yield surface of the Hoek-Brown constitutive model

As in the previous two cases, the plastic potential equation (g) has the same form as the model yield function (f) and differs by the dilation parameter m_{bdil} instead of the parameter m_b (Hoek, et al., 2002).

The quantity σ_{ci} in equations (5) and (6) represents the uniaxial compressive strength of the rock mass, while m_b, s and a are model parameters that are determined based on the intact rock parameters m_i and GSI, as well as the rock mass disturbance factor D (Hoek, et al., 2002).

Hyperbolic soil model

Granular unbound materials, such as coarse-grained sand and stone rubble, do not possess cohesion (c), so the shear strength of the soil can be defined by applying effective stresses in the form of an equation that defines the dependence of the shear stress at failure on the normal stress (Maksimović, 2008) by an equation of the form

$$\tau_f = \sigma_n \tan\phi(\sigma_n) \tag{7}$$

Unlike the Mohr-Coulomb and Matsuoka-Nakai models, where the angle of internal friction (ϕ) is a material parameter, in this constitutive model the angle of internal friction in the material is a function of the normal effective stress (Maksimović, 2008) and is defined by the equation

$$\phi(\sigma_n) = \phi_B + \delta\phi(\sigma_n) = \phi_B + \frac{\Delta\phi}{1+\frac{\sigma_n}{p_N}} \tag{8}$$

Considering the equation (8), the shear strength of the material (7) is defined by the equation

$$\tau_f = \sigma_n \tan\left(\phi_B + \frac{\Delta\phi}{1+\frac{\sigma_n}{p_N}}\right) \tag{9}$$

The quantities ϕ_B, $\Delta\phi$ and p_N in equations (8) and (9), represent the parameters of the constitutive model. The fracture surface of this constitutive model, in the stress space $\sigma - \tau$, is shown in **Fig. 4**.

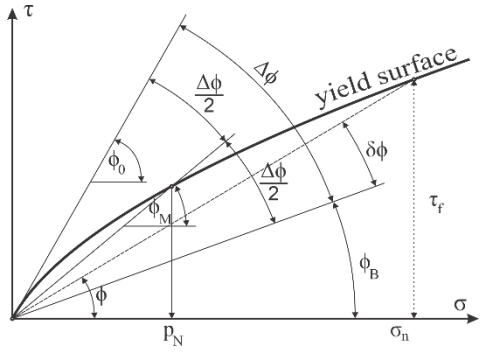

Fig. 4. Yield surface of the Hyperbolic soil model

Based on the previous discussion, it can be concluded that the equation of the yield surface of the hyperbolic soil model (7) corresponds to the equation of the yield surface of the Mohr-Coulomb model (1), with the fact that there is no material cohesion (c) and that the angle of internal friction (ϕ) is a function of stress. For this reason, the yield surface of this model can be expressed by using stress invariants, in a similar way as for the Mohr-Coulomb model, taking into account the previously mentioned specificities of the model, so that it reads

$$f = \frac{I_1}{3}\sin\phi(\sigma) + \sqrt{J_{2D}}\left(\cos\theta - \frac{1}{\sqrt{3}}\sin\theta\sin\phi(\sigma)\right) \tag{10}$$

In the case of considering the associative flow condition, the equations of the yield surface (f) and the plastic potential equation (g) differ, whereby the function of the Mohr-Coulomb model is most often used for the function of the plastic potential.

3. Implicit Stress Integration Procedure

3.1 General Algorithm for Implicit Stress Integration

Based on the incremental plasticity theory, if in the current configuration the stress point is below the yield surface, there is an increment of only elastic strain (Bathe, 1996). However, in the case when the stress point is located on the yield surface, in the current configuration, in addition to elastic strain, there is also an increase in plastic strain. In this case, the increment of the total strain can be represented as the sum of the elastic and plastic part of the strain, according to

$$d\mathbf{e} = d\mathbf{e}^E + d\mathbf{e}^P \tag{11}$$

The plastic strain increment vector has a direction normal to the surface of the plastic potential and is defined by the equation

$$d\mathbf{e}^P = d\lambda \frac{\partial g}{\partial \boldsymbol{\sigma}} \tag{12}$$

where $d\lambda$ is the so-called plastic multiplier, which needs to be determined. According to the theory of incremental plasticity, a condition must be met in each configuration

$$f \le 0, \quad d\lambda \ge 0, \quad f \cdot d\lambda = 0 \quad \text{and} \quad df = 0 \tag{13}$$

In order for relations (13) to be satisfied, in the case when the stress point is located below the yield surface, it is valid that $f < 0$, while in the case when the stress point is on the yield surface, the condition $(13)_3$ is valid, from which it follows

$$\frac{\partial f}{\partial \boldsymbol{\sigma}}^T d\boldsymbol{\sigma} + \frac{\partial f}{\partial \kappa}^T d\kappa = 0 \tag{14}$$

where κ is the so-called internal variable (variable based on plastic deformation, strain like) that exists in the case of models with deformation reinforcement.

As the stress is the result of purely elastic deformation, the stress increment in the current configuration can be calculated according to

$$d\boldsymbol{\sigma} = \mathbf{C}^E \left(d\mathbf{e} - d\mathbf{e}^P \right) \tag{15}$$

where $\mathbf{C}^E$ represents the elastic constitutive matrix (matrix of elastic coefficients).

Substituting equation (12) into (15) and then substituting it into (14), it becomes

$$df = \frac{\partial f}{\partial \boldsymbol{\sigma}}^T \left(\mathbf{C}^E d\mathbf{e} - d\lambda \mathbf{C}^E \frac{\partial g}{\partial \boldsymbol{\sigma}} \right) - d\lambda H = 0 \tag{16}$$

where H is the so-called hardening modulus.

Now from equation (16) the plastic multiplier $d\lambda$ can be calculated according to

$$d\lambda = \frac{\frac{\partial f}{\partial \boldsymbol{\sigma}}^T \mathbf{C}^E d\mathbf{e}}{H + \frac{\partial f}{\partial \boldsymbol{\sigma}}^T \mathbf{C}^E \frac{\partial g}{\partial \boldsymbol{\sigma}}} \tag{17}$$

on the basis of which, by applying (12), the increase in plastic strain can be calculated, so it is subtracted from the total strain, which gives the elastic part of the strain, and it is possible to calculate the stress.

Thus, the plastic strain increment direction is defined by the derivative of the plastic potential function with respect to stress, while the intensity of the plastic strain increment vector is defined by the plastic multiplier $d\lambda$. However, the plastic multiplier calculated in this way does not always ensure that the stress point is exactly on the yield surface, so it is necessary to slightly correct the value of the multiplier, for which the bisection method and Newton's method are most often used (De Souza Neto, et al., 2008; De Borst, et al., 2012).

4. Implementation in PAK program

The previously presented equations for the implicit integration of the stress of the constitutive models for soil and rock mass are summarized below in the form of a numerical algorithm shown in **Table 1**. The presented algorithm can be applied to all previously presented constitutive models, so this algorithm is implemented in the PAK program (Kojić, et al., 2011) in the form shown.

Known quantities: ${}^{t+\Delta t}\mathbf{e}$, ${}^{t}\mathbf{e}$, ${}^{t}\boldsymbol{\sigma}$, ${}^{t}\mathbf{e}^{P}$

A. Trial (elastic) solution for stress:

$d\boldsymbol{\sigma} = \mathbf{C}^{E} d\mathbf{e}^{E} = \mathbf{C}^{E}\left({}^{t+\Delta t}\mathbf{e} - {}^{t}\mathbf{e}\right)$, ${}^{t+\Delta t}\boldsymbol{\sigma} = {}^{t}\boldsymbol{\sigma} + d\boldsymbol{\sigma}$

Yield function calculation:

$f = f\left({}^{t+\Delta t}\sigma\right)$

B. Checking yield condition:

IF ($f < 0$) trial solutions are elastic (go to **E**)

IF ($f \geq 0$) elastic-plastic solutions (continue)

Calculation the derivatives:

$\frac{\partial f}{\partial \boldsymbol{\sigma}}$, $\frac{\partial g}{\partial \boldsymbol{\sigma}}$, $\frac{\partial \kappa}{\partial d\mathbf{e}^{P}}$

Plastic multiplier calculation

$$d\lambda = \frac{\frac{\partial f}{\partial \boldsymbol{\sigma}}^{T} \mathbf{C}^{E} d\mathbf{e}}{\frac{\partial f}{\partial \boldsymbol{\sigma}}^{T} \mathbf{C}^{E} \frac{\partial g}{\partial \boldsymbol{\sigma}} + H}$$

C. Local iterations by $d\lambda$ (using bisection method or Newton's method):

$d\mathbf{e}^{P} = d\lambda \frac{\partial g}{\partial \boldsymbol{\sigma}}$, $d\mathbf{e}^{E} = d\mathbf{e} - d\mathbf{e}^{P}$,

$d\boldsymbol{\sigma} = \mathbf{C}^{E} d\mathbf{e}^{E}$, ${}^{t+\Delta t}\boldsymbol{\sigma} = {}^{t}\boldsymbol{\sigma} + d\boldsymbol{\sigma}$

Yield function calculation:

$f = f\left({}^{t+\Delta t}\sigma\right)$

D. IF ($abs(f) \geq tol$) go to **C** with new $d\lambda$:

${}^{t+\Delta t}\mathbf{e}^{P} = {}^{t}\mathbf{e}^{P} + d\mathbf{e}^{P}$

E. Quantities at the end of the step: ${}^{t+\Delta t}\boldsymbol{\sigma}$, ${}^{t+\Delta t}\mathbf{e}^{P}$

Table 1. Implicit stress integration algorithm

Verification and Test Examples

Verification of the algorithm for the implicit stress integration of the presented constitutive models for soil and rock was performed through verification examples for each of the mentioned models. The results of numerical simulation of triaxial tests and direct shear tests on one hexahedral finite element of unit dimensions are presented below. Numerical simulations of the mentioned tests represent a simple way of verifying the constitutive models by comparing the results with analytical or experimental solutions of the given problem.

Triaxial test

The numerical model of the triaxial test on one finite element, with boundary conditions and loads, is shown in **Fig. 5**a. The load is given using the pressure on the free surfaces of the model, in all three coordinate directions.

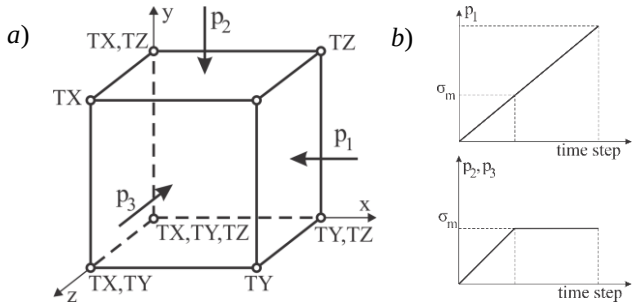

Fig. 5. Simulation of triaxial test and load functions

The pressure is applied in two phases: in the first phase (confining phase) of loading, a hydrostatic stress state is established, while in the second phase, the pressure components in two directions remaining the same, while the third component increases until the failure, which is manifested by the impossibility of achieving convergence. The numerical test, like the experiment, was carried out for five different levels of the confining stress.

Model	E (kN/m^2)	ν (-)	c (kN/m^2)	ϕ (°)	ϕ_b (°)	Δϕ (°)	p_n (kN/m^2)	σ_{ci} (kN/m^2)	m_b (-)	s (-)	a (-)
MC	100	0.25	0.20	7.0	-	-	-	-	-	-	-
Hyp	100	0.25	-	-	6.2	15.8	4.80	-	-	-	-
HB	300	0.25	-	-	-	-	-	23.0	0.481	$2.0x10^{-4}$	0.532

Table 2. Constitutive model parameters in triaxial test simulation

The load functions used in the numerical simulation are shown in **Fig. 5**b, while the parameters of the constitutive models, obtained by identification, are given in **Table 2**.

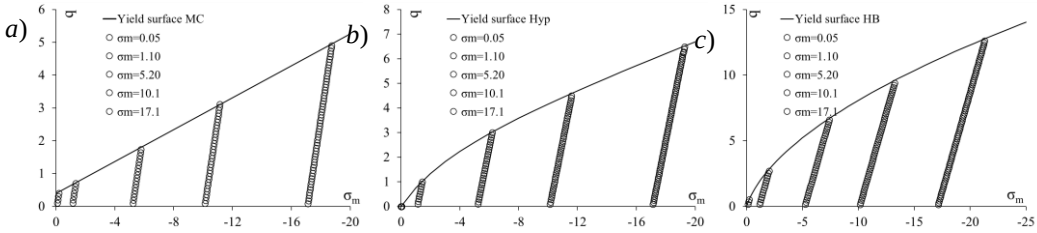

Fig. 6. Yield surface and stress path: a) Mohr-Coulomb, b) Hyperbolic soil and c) Hoek-Brown model

The results of the numerical simulation of the triaxial test are shown in **Fig. 6**. The figures show yield surfaces of different constitutive models and stress paths at different confining stress.

Based on the results shown in **Fig. 6**, it can be concluded that the developed and implemented algorithms provide theoretical values of stress at fracture, for each of the analyzed constitutive models, that is, numerical solutions were obtained in accordance with theoretical values of stress at failure, for different values of confining stress.

Direct shear test

The numerical model of the direct shear test, on one finite element, with boundary conditions and loads is shown in **Fig. 7**a.

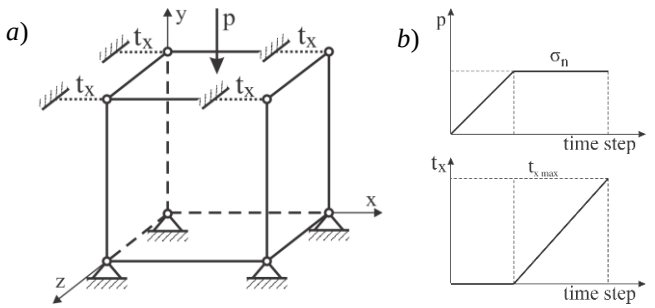

Fig. 7. Numerical simulation model of direct shear test and load function

The loading of the numerical model is given in two phases: in the first phase, the normal stress is given up to the stress level used in the experiment, after which shearing is performed, using the applied displacements. The load functions used in the numerical simulation are shown in **Fig. 7**b. The identification of the parameters of the constitutive models used in the numerical simulations was carried out by applying the results of material testing. The analyzed material is a rock pile, so constitutive models were used to simulate the mechanical behavior of granular materials, such as Mohr-Coulomb, Matsuoka-Nakai and the Hyperbolic soil model.

Using the measured values (Jaroslav Černi Water Institute, 1995) of normal and shear stress shown in **Fig. 8**, the model parameters were identified. The normal stress values shown are for use in the numerical simulation of the shear test.

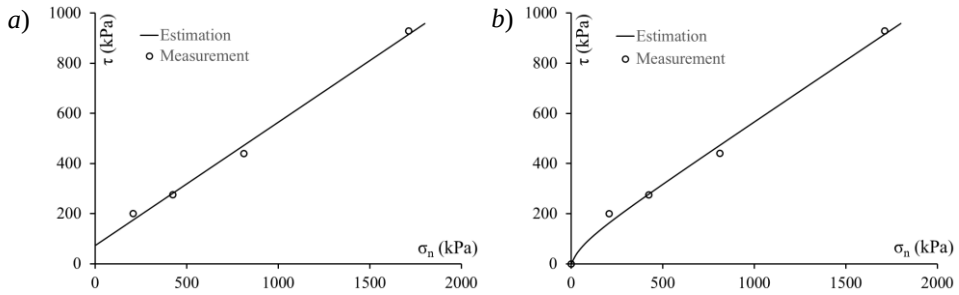

Fig. 8. Material parameter identification a) Mohr-Coulomb and b) Hyperbolic soil model

The result of identification using Mohr-Coulomb and Hyperbolic soil model is shown **Table 3**. The identified parameters were then used in the numerical simulation of the direct shear test using the finite element model shown in **Fig. 7**a.

Model	E (MN/m^2)	ν (-)	c (kN/m^2)	ϕ (°)	ϕ_b (°)	Δϕ (°)	p_n (kN/m^2)
MC	100	0.30	72.6	26.2	-	-	-
Hyp	100	0.30	-	-	25.9	35.1	112.0

Table 3. Constitutive model parameters in direct shear test simulation

The results of the numerical simulation, together with the test results (Jaroslav Černi Water Institute, 1995), are shown in **Fig. 9**. By analyzing the results obtained by applying these models, a good agreement with the results of experimental tests of the samples can be observed, for all values of the normal stress.

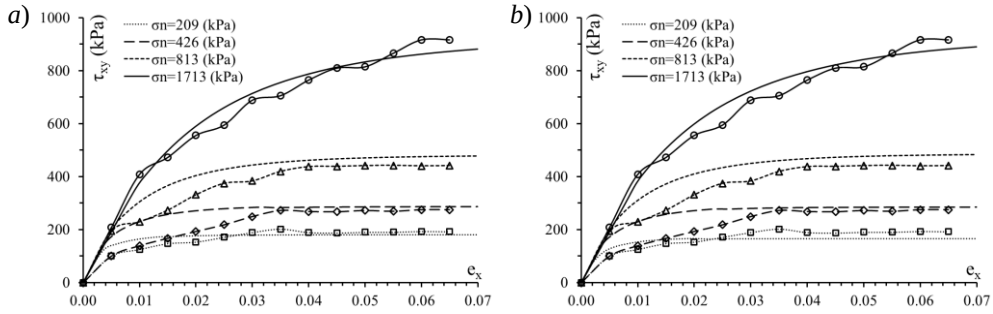

Fig. 9. Direct shear test using a) Mohr-Coulomb and b) Hyperbolic soil model

This confirms that even on the basis of a relatively simple shear test, the parameters of the constitutive model can be identified for use in numerical simulations of real problems. It can also be concluded that the developed algorithms of the constitutive models describe well the mechanical behavior of the analyzed samples of granular materials, such as rock piles.

In order to further increase the accuracy of numerical simulations, it is possible to additionally calibrate the parameters of the constitutive models thus adopted. In this way, the deviations of the mechanical behavior of numerical models from the behavior of real material samples can be minimized.

4. Conclusions

This paper presents an implicit stress integration procedure for selected soil and rock constitutive models, including Mohr-Coulomb, Matsuoka-Nakai, Hyperbolic soil model, and Hoek-Brown model. Based on the theory of incremental plasticity, equations for implicit stress integration were derived. The implementation of the developed algorithm was carried out within the PAK software package, which gave it advanced possibilities of simulating the mechanical behavior of geomaterials. The verification of the implemented models was carried out through the simulation of triaxial tests and direct shear tests, and the obtained results showed a good agreement with theoretical and experimental values. This confirmed the accuracy and reliability of the developed numerical procedures, as well as their applicability in engineering practice. Further directions of development include expanding the library of constitutive models to models that include anisotropy, viscosity and damage, which would further increase the precision and universality of numerical analyzes in the PAK software package for the field of geotechnics.

Acknowledgements: This research is partly supported by the Ministry of Education and Science, Republic of Serbia, Grant TR32036 and Grant TR37013.

References

Balmer, G., 1952. A general analytical solution for Mohr's envelope. *Proceedings of American Society for Testing and Materials, vol. 52,* pp. 1260-1271.

Bathe, K. J., 1996. *Finite Element Procedures.* USA: Massachusetts Institute of Technoogy.

De Borst, R., Crisfield, M. A., Remmers, J. J. & Verhoosel, C. V., 2012. *Nonlinear finite element analysis of solids and structures, 2nd ed.*. Chichester: John Wiley & Sons.

De Souza Neto, E. A., Perić, D. & Owen, D. R., 2008. *Computational methods for plasticity: theory and applications.* Chichester: John Wiley & Sons.

Hoek, E., 2007. *Practical rock engineering.* North Vancouver, Canada: Evert Hoek Consulting Engineer Inc..

Hoek, E., Carranza-Torres, C. & Corkum, B., 2002. *Hoek-Brown failure criterion - 2002 edition.* Toronto, Canada, s.n., pp. 267-273.

Jaroslav Černi Water Institute, 1995. *Shear test report on a large scale (on Serbian),* Belgrade: Jaroslav Černi Water Institute.

Kojić, M., Slavković, R., Živković, M. & Grujović, N., 2011. *PAK-S: Program for FE Structural Analysis,* Kragujevac: University of Kragujevac, Faculty of Engineering.

Maksimović, M., 2008. *Mehanika tla, četvrto izdanje.* Beograd: AMG knjiga.

Matsuoka, H. & Nakai, T., 1974. Stress–deformation and strength characteristics of soil under three different principal stresses. *Proceedings of the Japan Society of Civil Engineers,* Tom 232, pp. 59-70.

Matsuoka, H., Sun, A. & Konda, T., 1994. *A constitutive law from frictional to cohesive materials.* New Delhi, s.n.

Smith, I. & Griffiths, V., 2004. *Programming the Finite Element Method.* England: John Wiley & Sons Ltd.